

## A whispering gallery mode microsphere resonator coupled by anti-resonant reflecting guidance mechanism

WU Jie-Ya<sup>1</sup>, WANG Dong-Ning<sup>1,2\*</sup>, ZHAO Chun-Liu<sup>1\*</sup>

- (1. College of Optical and Electronic Technology, China Jiliang University, Hangzhou 310018, China;  
2. College of Urban Transportation and Logistics, Shenzhen Technology University, Shenzhen 518118, China)

**Abstract:** A whispering gallery mode microsphere resonator is proposed and demonstrated. The device is fabricated by splicing a single-mode fiber with a capillary tube and, by properly adjusting the discharging current and the splicing position of the fiber and capillary tube, an expanded hollow sphere cavity is formed at the splicing junction. A microsphere is inserted into the hollow sphere cavity and positioned in close touch with the cavity wall to excite whispering gallery mode resonance via the coupling of the evanescent field of the anti-resonant reflecting guidance mode produced in the cavity wall. The device has a quality factor of  $3.725 \times 10^3$  and is compact, simple in fabrication, easy in packaging, convenient in operation and of low cost.

**Key words:** resonator, microcavity, optical fiber device

## 反谐振反射模式耦合的回音壁模式微球谐振器

武洁雅<sup>1</sup>, 王东宁<sup>1,2\*</sup>, 赵春柳<sup>1\*</sup>

- (1. 中国计量大学 光电学院, 浙江 杭州 310018;  
2. 深圳技术大学 城市交通与物流学院, 广东 深圳 518118)

**摘要:** 本文提出并演示了一种回音壁模式微球谐振器。该装置的制备是将单模光纤与毛细管熔接, 通过适当调节放电电流和光纤与毛细管的熔接位置, 形成一个膨胀的空心球腔。微球被插入空心球腔中, 并与腔壁紧密接触, 通过渐逝场的耦合在腔壁中产生的反谐振导向机制来激发回音壁模式共振。该设备的品质因数为  $3.725 \times 10^3$ , 结构紧凑, 制造简单, 易于封装, 操作方便, 成本低。

**关键词:** 谐振器; 微腔; 光纤器件

中图分类号: TN253

文献标识码: A

### Introduction

Whispering gallery mode (WGM) is the specific resonance (or mode) of a wave field that is confined inside a given resonator by using the continuous total internal reflection (TIR). A WGM resonator has a high  $Q$ -factor (or narrow linewidth) and a small mode volume, hence supporting widespread applications in sensors, filters, microlasers, and modulators<sup>[1-5]</sup>. The common WGM excitation schemes are generally based on phase-matching of the evanescent fields, to couple light from the outside into the WGM resonators. Currently, the main coupling techniques include prism, planar waveguide, side pol-

ished or angle polished optical fiber, and tapered optical fiber<sup>[6-10]</sup>. The prism coupling is a flexible and efficient means for free space optical operation, but it involves with bulky components and needs a careful alignment. Planar waveguide coupling is compact and robust; however, it requires high precision and complicated fabrication techniques and is not compatible with optical fiber. Although the side polished or angle polished fiber coupling is compatible with optical fiber and convenient for use, its fabrication is relatively difficult and the coupling efficiency is relatively low. The highest coupling efficiency can be realized by using the tapered optical fiber coupling; however, the tapered fiber is fragile in structure,

Received date: 2025-03-11, accepted date: 2025-07-11

收稿日期: 2025-03-11, 录用日期: 2025-07-11

Foundation items: Supported by the National Natural Science Foundation of China (61975192); the National Key Research and Development Project of China (2020YFF0217801); the Open fund of Guangdong provincial key laboratory of information photonics technology (GKPT20-04)

Biography: WU Jie-Ya (1997—), female, Anhui, master. Research field is optical fiber sensing. Email: 2279118850@qq.com

\*Corresponding authors: Email: wangdongning@sztu.edu.cn; clzhao@cjlu.edu.cn

which results in long term operation instability of the device.

WGM resonators based on the commercially available microsphere are featured with high compactness, flexible and convenient operation and low cost, and have attracted a lot of research attention in recent years. A WGM microsphere resonator is suitable for the coupling schemes such as the use of chemically etched photonic crystal fiber (PCF) or capillary tube, and tapered hollow annular core fiber<sup>[11-14]</sup>. However, the etched PCF and capillary are fragile and, for the tapered hollow annular core fiber, the WGM resonance is relatively weak due to strong reflection from the Fabry-Perot (FP) cavity.

In this paper, a new coupling method for WGM microsphere resonator is proposed and demonstrated by using the anti-resonant reflecting guidance (ARRG) mechanism<sup>[15-16]</sup>, which is an effect that causes the lossy dips in the transmission spectrum. The device consists of a single-mode fiber (SMF) connected with an expanded hollow sphere cavity of capillary tube, formed in the fusing splicing process. The wall of the hollow sphere cavity can be considered as an FP etalon. Wavelengths that satisfy the resonant condition will leak out of the wall, whereas the other wavelengths can continue to propagate in the wall of capillary tube as the guide modes. When the incident light arrives at the interface of SMF and the hollow sphere cavity, part of the light enters the wall of the hollow sphere cavity, and propagates along the wall by following the total internal reflection. When the light path is tangential with the microsphere surface at the contacting point, it is coupled into the microsphere and excites WGM if the phase matching condition can be satisfied. Such a WGM microsphere resonator is compact in size, simple in fabrication, low in cost and convenient in operation and has a quality ( $Q$ ) factor of  $3.725 \times 10^3$ .

## 1 Device fabrication

The proposed optical fiber WGM microsphere resonator consists of an SMF and a capillary tube, both are fusion spliced to form an expanded hollow sphere cavity. A microsphere is adhered to the inner wall of the hollow sphere cavity with the help of a tapered fiber.

The fabrication process of the device is illustrated in Fig. 1. Firstly, a section of capillary tube with an outer diameter of  $149 \mu\text{m}$ , an inner diameter of  $75 \mu\text{m}$  and a length of  $800 \mu\text{m}$  is fusion spliced with an SMF, as shown in Fig. 1(a). The other end of the capillary tube is fusion spliced with another section of SMF as shown in Fig. 1(b). By continuously adjusting the splicing position of the capillary tube and the SMF until part of the capillary tube collapses and expands into a hollow sphere cavity with a wall thickness of  $\sim 15 \mu\text{m}$ , as shown in Fig. 1(c). Due to the collapse of the capillary tube at the SMF-capillary tube junction, a thin layer is formed. Next, the capillary tube is cut away at a position distant from the hollow sphere cavity, as shown in Fig. 1(d).

A tapered optical fiber covered with a thin layer of UV adhesive is then used to push a microsphere (Cospheric Inc, BTGMS-4.21, barium titanate) with a di-

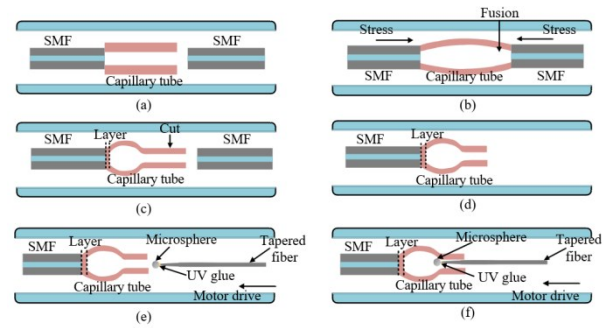


Fig. 1 Schematic diagrams of the fabrication process of the WGM microsphere resonator: (a) one end of the capillary tube is fusion spliced with an SMF; (b) the other end of the capillary tube is fusion spliced with another SMF; (c) the hollow sphere cavity is formed by continuously discharging the SMF-capillary tube junction; (d) the capillary tube is cut at a position distant from the hollow sphere cavity; (e) a tapered fiber covered with UV glue is used to insert the microsphere into the hollow sphere cavity by using a motor drive; (f) the microsphere is positioned in close touch with the inner wall of the hollow sphere cavity

图1 WGM微球谐振器制备示意图:(a)毛细管的一端与单模光纤熔接;(b)毛细管的另一端与另一段单模光纤熔接;(c)通过在单模光纤毛细管连接处连续放电形成空心球腔;(d)在远离空心球腔的位置切割毛细管;(e)使用覆盖有紫外胶的锥形光纤,通过使用电机驱动器将微球插入空心球腔内;(f)微球放置在与空心球腔的内壁紧密接触的位置

ameter of  $\sim 73 \mu\text{m}$  into the capillary tube and then the hollow sphere cavity, as shown in Fig. 1(e).

The position of the microsphere in close touch with the inner wall of the hollow sphere cavity is continuously adjusted by using the tapered fiber as shown in Fig. 1(f), until the WGM resonance appears in the reflection spectrum of the device. The UV adhesive is then solidified by UV light illumination, to provide a robust structure of the WGM resonator.

The function of tapered fiber is to help adjust the position of the microspheres in the cavity to allow light to be coupled into the microspheres efficiently, thereby exciting the WGM resonance.

The microscope image of the fabricated WGM microsphere resonator is displayed in Fig. 2.

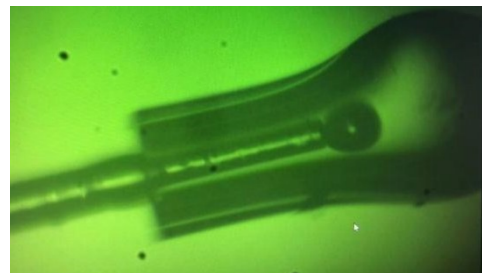


Fig. 2 Microscope image of the WGM microsphere resonator  
图2 回音壁模式微球谐振腔的显微图像

## 2 Operation principle

The operation principle of the device is illustrated in Fig. 3, where it can be observed that there are five possi-

ble reflection surfaces:  $S_1$ ,  $S_2$ ,  $S_3$ ,  $S_4$  and  $S_5$  respectively. The front and back surfaces of the thin layer at the SMF-capillary tube junction,  $S_1$  and  $S_2$ , the front and back surfaces of microsphere  $S_3$  and  $S_4$ , and the end face of the capillary tube,  $S_5$ .

Part of the incident light traveling along the core of SMF is directed into the wall of hollow sphere cavity, and propagates along the cavity wall by experiencing total internal reflection. When the light beam traveling along the wall follows the tangential path of the microsphere, it is coupled into the microsphere at the contacting point, and circulates along the microsphere surface, hence exciting the WGM resonance. After propagating along the surface of the microsphere for a period, the light beam leaves the microsphere and propagates along the wall of capillary tube, until it is reflected at the cutting end surface of the capillary tube and finally returns to the core of SMF.

The rest part of the light is reflected sequentially at the thin layer surfaces and the microsphere surfaces, and as a result, a cascaded FP interferometer is formed, which may include an FP cavity formed by the surfaces of  $S_1$  and  $S_2$ ,  $S_2$  and  $S_3$ , and  $S_3$  and  $S_4$ , with cavity lengths of  $L_{\text{layer}}$ ,  $L_{\text{air}}$  and  $L_m$ , respectively, as shown in Fig. 3.

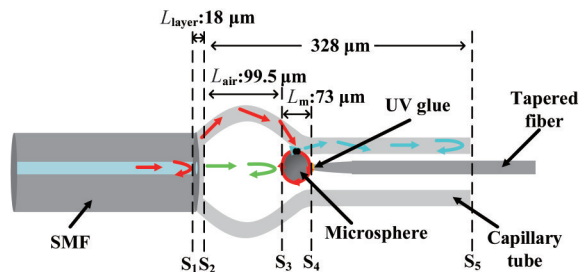


Fig. 3 Schematic diagram of the WGM microsphere resonator  
图3 回音壁模式微球谐振器示意图

The microscope image of the device under red light illumination is displayed in Fig. 4, where the high reflection at the end of capillary tube reveals the ARRG mechanism existed<sup>[16]</sup>. It can also be observed from the figure that the light circulates along the circumference of the microsphere, which confirms the existence of the WGM resonance.

The free spectral range (FSR) of the spectrum is

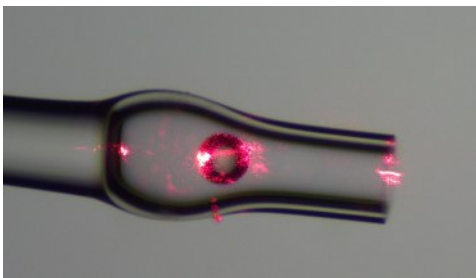


Fig. 4 Microscope image of the device under red light illumination  
图4 器件在红光照射下的显微镜图像

given by:

$$\text{FSR} = \frac{\lambda_1 \lambda_2}{\text{OPD}} = \frac{1}{f}, \quad (1)$$

where  $\lambda_1$  and  $\lambda_2$  represent the adjacent resonance peak wavelengths, OPD is the optical path difference produced, and  $f$  is the corresponding spatial frequency.

For a WGM microsphere resonator:

$$\text{OPD}_{\text{WGM}} = n_m \pi D, \quad (2)$$

where  $n_m$  is the refractive index and  $D$  is the diameter of the microsphere.

For an FP cavity:

$$\text{OPD}_{\text{FP}} = 2nL, \quad (3)$$

where  $n$  is the refractive index of the FP cavity medium, and  $L$  is the FP cavity length.

Since FSR is the reciprocal of the spatial frequency and the cavity lengths are known, the OPD or the actual spatial frequency corresponding to each frequency peak can be calculated and used to determine whether the structure operates in a WGM mode or an FP mode, or both.

### 3 Experiment and discussion

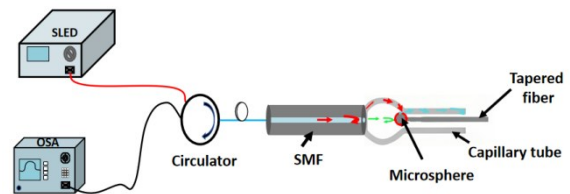


Fig. 5 Schematic of the experimental setup  
图5 实验装置示意图

To demonstrate the operation of the proposed device, the reflection spectrum of the WGM microsphere resonator needs to be recorded and the experimental setup is shown in Fig. 5. The light from a broadband light source (Haoyuan Optoelectronics, HY-SLE) is introduced into the device through a circulator. The reflected light from the device is directed to the output port of the circulator and received by an optical spectrum analyzer (YOKOGAWA, AQ6370) with a resolution of 0.02 nm for recording the reflection spectrum.

The reflection spectrum of the expanded hollow sphere cavity device without the microsphere is displayed in Fig. 6(a). When the microsphere is inserted, the reflection spectrum of the device is shown in Fig. 6(b), and the corresponding spatial frequency spectrum obtained by implementing fast Fourier transform (FFT) is shown in Fig. 6(c). It can be observed from Fig. 6(c) that a number of peaks A, B, C, D, and E exist in the spatial frequency spectrum, situated at  $0.0249 \text{ nm}^{-1}$ ,  $0.0833 \text{ nm}^{-1}$ ,  $0.1916 \text{ nm}^{-1}$ ,  $0.2749 \text{ nm}^{-1}$  and  $0.2916 \text{ nm}^{-1}$  respectively. The OPD value corresponding to the frequency peak A is  $\sim 59.8 \mu\text{m}$ , which is close to the OPD value of  $51.8 \mu\text{m}$  for the FP cavity formed by the reflection surfaces of the thin layers,  $S_1$  and  $S_2$ , as the refractive index of the capillary tube is 1.44. The OPD value

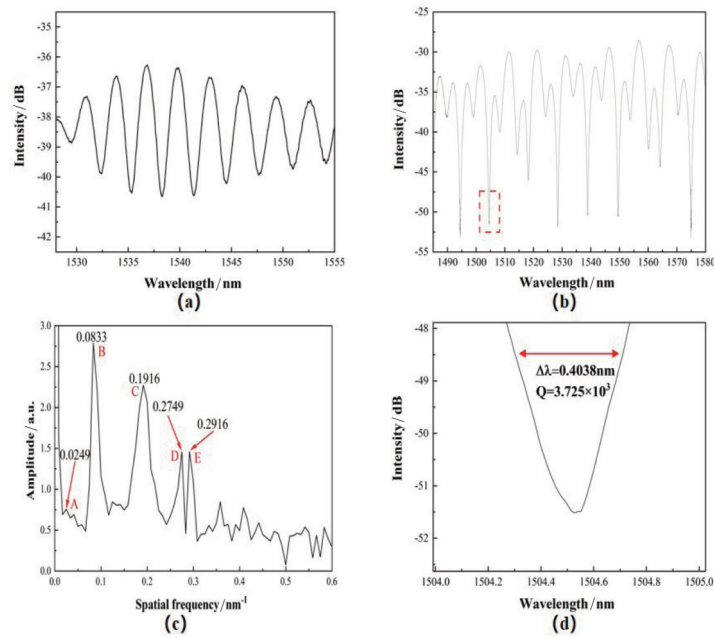


Fig. 6 (a) Reflection spectrum of the hollow sphere cavity without inserting the microsphere; (b) reflection spectrum of the WGM microsphere resonator; (c) FFT of the reflection spectrum; (d) enlarged view of the dotted box in the reflection spectrum of the WGM microsphere resonator

图6 (a)未插入微球的空心球腔的反射谱;(b)回音壁模式微球谐振器的反射谱;(c)反射谱的快速傅里叶变换;(d)回音壁模式微球谐振器反射谱中虚线框部分的放大图

corresponding to the frequency peak B is  $\sim 200.1 \mu\text{m}$ , which is close to the OPD value of  $199 \mu\text{m}$  for the air FP cavity formed by the reflection surfaces of  $S_2$  and  $S_3$ . Since the refractive index of the microsphere is 1.93 and the diameter is  $\sim 73 \mu\text{m}$ , according to Eq. (2), the corresponding OPD value of the WGM microsphere resonator can be calculated to be  $\sim 442.4 \mu\text{m}$ , which is close to the OPD value corresponding to the frequency peak C,  $\sim 460.3 \mu\text{m}$ . Thus our proposed device is indeed a WGM microsphere resonator. Figure 6(d) provides an enlarged view of the dashed box in Fig. 6(b). At the resonance wavelength of  $1504 \text{ nm}$ , the full-width at half maximum (FWHM) value of the main resonance is  $\sim 0.4038 \text{ nm}$ , and the  $Q$  factor can be determined as  $3.725 \times 10^3$ . Such a value is slightly better than that reported in Ref. [11], but is still lower than those in Refs. [12-14]. However, our device has a good robustness due to etching free, and the WGM resonance can be easily established.

The frequency peak D is the sum frequency of peak B and peak C ( $0.0833 + 0.1916 = 0.2749$ ) and the frequency peak E is the sum of peak D and peak A ( $0.2749 + 0.0249 = 0.2998$ ). It can also be noticed that the FP resonance between  $S_3$  and  $S_4$  is not found in Fig. 6(c), which is likely due to the weak reflection from the microsphere surfaces.

The device can be used for gas pressure measurement. When the external refractive index varies, the OPD related to the WGM microsphere resonator also changes, thus shifting the reflection spectrum. Considering the refractive index of the microsphere of 1.93 and the measured  $Q$  value of  $3.725 \times 10^3$ , the refractive index sensitivity that can be achieved in the device is in the or-

der of  $10^{-4}$ .

## 4 Conclusion

In conclusion, an optical fiber WGM microsphere resonator is demonstrated. The device is fabricated by fusion splicing SMF with a section of the capillary tube, which is expanded into a hollow sphere cavity at the SMF-capillary tube junction produced due to the high temperature during the splicing process. A microsphere is inserted into the hollow sphere cavity and in close touch with the cavity wall to excite the WGM through the evanescent field coupling between the microsphere and the cavity wall due to the anti-resonant reflecting guidance mechanism. The device has a good  $Q$ -factor of  $3.725 \times 10^3$  and is compact, simple in fabrication, easy in packaging, convenient in operation and of low cost.

## References

- [1] Matsko A B, Ilchenko V S. Optical resonators with whispering-gallery modes—part I: basics [J]. IEEE Journal of Selected Topics in Quantum Electronics, 2006, 12(1): 3–14.
- [2] Ilchenko V S, Matsko A B. Optical resonators with whispering-gallery modes—part II: applications [J]. IEEE J. Sel. Topics Quantum Electron, 2006, 12: 15–32.
- [3] Ward J, Benson O. WGM microresonators: sensing, lasing and fundamental optics with microspheres [J]. Laser & Photonics Reviews, 2011, 5(4): 553–570.
- [4] Soria S, Berneschi S, Brenci M, et al. Optical microspherical resonators for biomedical sensing [J]. Sensors, 2011, 11(1): 785–805.
- [5] Lin J T, Xu Y X, Song J X, et al. Low-threshold whispering-gallery-mode microlasers fabricated in a Nd: glass substrate by three-dimensional femtosecond laser micromachining [J]. Optics Letters, 2013, 38(9): 1458–1460.
- [6] Mazzei A, Göttinger S, Menezes L S, et al. Optimization of prism coupling to high-Q modes in a microsphere resonator using a near-field probe [J]. Optics Communications, 2005, 250(4–6): 428–433.

- [7] Xifré-Pérez E, Domenech J D, Fenollosa R, et al. All silicon waveguide spherical microcavity coupler device [J]. *Optics Express*, 2011, 19(4): 3185–3192.
- [8] Dubreuil N, Knight J, Leventhal D K, et al. Eroded monomode optical fiber for whispering-gallery mode excitation in fused-silica microspheres [J]. *Optics Letters*, 1995, 20(8): 813–815.
- [9] Knight J C, Cheung G, Jacques F, et al. Phase-matched excitation of whispering-gallery-mode resonances by a fiber taper [J]. *Optics Letters*, 1997, 22(15): 1129–1131.
- [10] Milenko K, Konidakis I, Pissadakis S. Silver iodide phosphate glass microsphere resonator integrated on an optical fiber taper [J]. *Optics Letters*, 2016, 41(10): 2185–2188.
- [11] Kosma K, Zito G, Schuster K, et al. Whispering gallery mode microsphere resonator integrated inside a microstructured optical fiber [J]. *Optics Letters*, 2013, 38(8): 1301–1303.
- [12] Shi L L, Zhu T, Huang D M, et al. Thermo-optic tuning of integrated polymethyl methacrylate sphere whispering gallery mode resonator [J]. *IEEE Photonics Journal*, 2016, 8(5): 2701307–1–2701307–7.
- [13] Zhang X B, Yang Y, Shao H Y, et al. Fano resonances in cone-shaped inwall capillary based microsphere resonator [J]. *Optics Express*, 2017, 25(2): 615–621.
- [14] Wang J, Zhang X, Yan M, et al. Embedded whispering-gallery mode microsphere resonator in a tapered hollow annular core fiber [J]. *Photon. Res.*, 2018, 6(12): 1124–1129.
- [15] Hou M X, Zhu F, Wang Y, et al. Antiresonant reflecting guidance mechanism in hollow-core fiber for gas pressure sensing [J]. *Optics Express*, 2016, 24(24): 27890–27898.
- [16] Yang Y B, Wang D N, Xu B, et al. Optical fiber tip interferometer gas pressure sensor based on anti-resonant reflecting guidance mechanism [J]. *Optical Fiber Technology*, 2018, 42(5): 11–17.